

Nature of $X(3872)$ from data

Yu. S. Kalashnikova and A. V. Nefediev

Institute of Theoretical and Experimental Physics, 117218, B. Cheremushkinskaya 25, Moscow, Russia
 (Received 28 July 2009; published 2 October 2009)

Properties of the charmoniumlike state $X(3872)$ are investigated and its nature is discussed as based on the existing experimental data. In particular, we analyze the new data from Belle and *BABAR* Collaborations and argue that, while the *BABAR* data prefer the dynamically generated virtual state in the $D\bar{D}^*$ system, the new Belle data clearly indicate a sizable $c\bar{c}2^3P_1$ component in the X wave function.

DOI: 10.1103/PhysRevD.80.074004

PACS numbers: 14.40.Gx, 12.39.Mk, 12.39.Pn, 13.25.Gv

I. INTRODUCTION

In a few recent years a number of new states in the spectrum of charmonium have been found experimentally. These states, labeled as X 's, Y 's, and Z 's attract special attention of phenomenologists since most of them (if not all) can hardly fit into the standard quark model scheme. This means that, in addition to the genuine $c\bar{c}$ component, the wave functions of these states must have extra components, whose nature is not yet clear and is an open problem. Although various scenarios are suggested and discussed in the literature, such as threshold phenomena, hadronic molecule, and so on, no unambiguous criteria which would allow one to distinguish between different assignments for these "homeless" charmonia have been established so far.

Among these new charmoniumlike states the $X(3872)$ meson is most well-studied. The X was first observed in 2003 by the Belle Collaboration in charged B -meson decays $B \rightarrow KX$, in the mode $\pi^+\pi^-J/\psi$ [1], with the dipion originated from the ρ -meson. The mass and the width of the $X(3872)$ reported in Ref. [1] were

$$M_X = 3872.0 \pm 0.6(\text{stat}) \pm 0.5(\text{syst}) \text{ MeV} \quad (1)$$

and

$$\Gamma_X < 2.3 \text{ MeV}. \quad (2)$$

Later Belle reported their observation of the same state in the $\pi^+\pi^-\pi^0J/\psi$ ($\omega J/\psi$) and $\gamma J/\psi$ modes [2], with branching fractions

$$\text{Br}(B \rightarrow KX)\text{Br}(X \rightarrow \gamma J/\psi) = (1.8 \pm 0.6 \pm 0.1) \times 10^{-6}, \quad (3)$$

$$\frac{\text{Br}(X \rightarrow \pi^+\pi^-\pi^0J/\psi)}{\text{Br}(X \rightarrow \pi^+\pi^-J/\psi)} = 1.0 \pm 0.4 \pm 0.3, \quad (4)$$

$$\frac{\text{Br}(X \rightarrow \gamma J/\psi)}{\text{Br}(X \rightarrow \pi^+\pi^-J/\psi)} = 0.14 \pm 0.05. \quad (5)$$

The $X(3872)$ was confirmed in the discovery mode by the CDF [3], D0 [4], and *BABAR* [5] Collaborations. In

their recent updates, *BABAR* [6] and Belle [7] reduced slightly the branching ratio,

$$\text{Br}(B^+ \rightarrow K^+X)\text{Br}(X \rightarrow \pi^+\pi^-J/\psi) = (7 \div 10) \times 10^{-6}, \quad (6)$$

and both Belle and *BABAR* also observed the X in the B^0 decays with the rate comparable with the charged channel [6,7]. In addition, *BABAR* measured other decay modes of the X [8]:

$$\frac{\text{Br}(X \rightarrow \gamma J/\psi)}{\text{Br}(X \rightarrow \pi^+\pi^-J/\psi)} = 0.33 \pm 0.12, \quad (7)$$

$$\frac{\text{Br}(X \rightarrow \gamma \psi')}{\text{Br}(X \rightarrow \pi^+\pi^-J/\psi)} = 1.1 \pm 0.4, \quad (8)$$

and imposed the upper limit on the X production [9]:

$$\text{Br}(B \rightarrow KX) < 3.2 \cdot 10^{-4}. \quad (9)$$

The most recent CDF result for the mass of the X observed in the $\pi^+\pi^-J/\psi$ mode [10] is

$$M_X = 3871.61 \pm 0.16 \pm 0.19 \text{ MeV}. \quad (10)$$

Finally, the quantum numbers $J^{PC} = 1^{++}$ are favored for the X (although 2^{-+} are not yet excluded) [11].

Clearly the measured properties of the $X(3872)$ raise a number of questions concerning its nature. In particular, although the X is produced in the B -meson decays with the branching ratio of order 10^{-4} —see Eq. (9), that is with the branching ratio typical for genuine charmonia (such as J/ψ , ψ' , or χ_{c1}) [12], quark models fail to predict the existence of a $^3P_1 c\bar{c}$ meson in the vicinity of the observed mass of 3872 MeV (see, for example, [13]). In addition, quark-antiquark interpretation of the X faces a further challenge, namely, a strong isospin violation—see Eq. (4).

In the meantime, the observed mass of the $X(3872)$ measured in the $\pi^+\pi^-J/\psi$ channel, appears to be quite close to the position of the $D^0\bar{D}^{*0}$ threshold which, according to the most recent CLEO data [14] lies at

$$M_{D^0\bar{D}^{*0}} = 3871.81 \pm 0.36 \text{ MeV}. \quad (11)$$

It is quite natural to assume then that the X wave function contains a large admixture of the $D\bar{D}^*$ molecule component,¹ and the isospin violation is readily explained as due to the large (about 7 MeV) mass difference between the charged and neutral $D\bar{D}^*$ thresholds. Indeed, if one assumes that the decays $X \rightarrow \rho J/\psi$ and $X \rightarrow \omega J/\psi$ proceed via $D\bar{D}^*$ loops, then the isospin violation happens due to the difference between the charged and neutral loops which, in turn, is due to the aforementioned mass difference. Although it is not large *per se*, it is enhanced due to kinematical reasons, as the effective phase space available in case of the ρ is much larger than that in case of the ω [15,16].

To summarize, data seem to indicate a dynamical origin of the X . From the theoretical point of view several assignments for the latter are discussed in the literature.

It was noticed long ago [17] that one-pion exchange can be responsible for the formation of near-threshold states in D -meson systems. In particular, one-pion exchange is attractive in the $1^{++} D\bar{D}^*$ channel [17–20]. The $X(3872)$ as a virtual state was discussed in Ref. [16], as generated dynamically from the interaction of pseudoscalar and vector mesons.

On the other hand, in Ref. [21], in the framework of a coupled-channel microscopic quark model with the $c\bar{c} - D\bar{D}^*$ mixing, the $X(3872)$ is generated as a virtual state in the $D\bar{D}^*$ channel together with the 2^3P_1 charmonium resonance. Similar phenomenon is found in a coupled-channel analysis [22], where a more sophisticated QCD-motivated approach to light-quark pair creation is developed.

The X as a loosely $D\bar{D}^*$ bound state is advocated in Refs. [23,24], while the cusp scenario for the $\pi^+\pi^-J/\psi$ excitation curve in the $X(3872)$ mass range is discussed in Ref. [25].

Meanwhile, although the molecule assignment for the X seems to be quite plausible, it meets certain obstacles as well. To begin with, a natural worry is that in the $D\bar{D}^*$ system, bound by the one-pion exchange, the pion may go on-shell and thus binding may not be strong enough [15]. For the most recent work on the possibility for one-pion exchange to bind the $D\bar{D}^*$ system see [26,27]. Further implications of the nearby pion threshold are discussed in Refs. [28,29].

Furthermore, quite a large branching ratio for the radiative decay $X \rightarrow \gamma\psi'$ [see Eq. (8)] can be explained naturally in the framework of quark models. Indeed, it is well-known that in so-called Coulomb + linear quark potential models the radiative decay $\chi'_{c1} \rightarrow \gamma J/\psi$ is suppressed in comparison with decay $\chi'_{c1} \rightarrow \gamma\psi'$. For example, the estimates of Refs. [13,30] yield:

$$\begin{aligned} \Gamma(\chi'_{c1} \rightarrow \gamma J/\psi) &= 70 \text{ keV} [13], \quad 11 \text{ keV} [30], \\ \Gamma(\chi'_{c1} \rightarrow \gamma\psi') &= 180 \text{ keV} [13], \quad 64 \text{ keV} [30]. \end{aligned} \quad (12)$$

an opposite pattern was found in Ref. [19], and a large $\gamma\psi'$ rate is now considered as an evidence against the molecule interpretation. Notice, however, that there exists a mechanism for the radiative decays of molecules via $D^{(*)}$ -meson loops which was not considered in Ref. [19] and which favors the $\chi'_{c1} \rightarrow \gamma\psi'$ decay rate over the $\chi'_{c1} \rightarrow \gamma J/\psi$ one. However, a reliable evaluation of such radiative decays of molecules meets severe problems with divergent loop integrals which can hardly be resolved in a model-independent way.

Finally, for a pure molecule, the branching fraction $B \rightarrow KX$ was estimated in Ref. [31] to be less than 10^{-5} , that is much smaller than the experimental data on the X production (though, being very model-dependent, such estimates should be treated with caution). So it seems quite reasonable to assume that this is the $c\bar{c}$ component of the X to be responsible for the X production in B meson decays and for the X radiative decays.

The interest to the $X(3872)$ was catalyzed even more in 2006, when Belle reported an enhancement of the $D^0\bar{D}^0\pi^0$ signal just above the $D^0\bar{D}^{*0}$ threshold observed in the reaction $B^+ \rightarrow K^+ D^0\bar{D}^0\pi^0$ [32,33] at

$$M_X = 3875.2 \pm 0.7_{-1.6}^{+0.3} \pm 0.8 \text{ MeV}, \quad (13)$$

with the branching

$$\text{Br}(B^+ \rightarrow K^+ D^0\bar{D}^0\pi^0) = (1.02 \pm 0.31_{-0.29}^{+0.21}) \times 10^{-4}. \quad (14)$$

The corresponding state was called the $X(3875)$ and it was confirmed later by the *BABAR* Collaboration as well [34].

Although an immediate and the most natural conclusion is that this is simply yet another manifestation of the same well-established state $X(3872)$, a 3 MeV shift in the mass may have had dramatic consequences for such an interpretation. As a result, a rather extreme assumption was made that two different charmoniumlike states might reside in the same mass region. It was noticed in Ref. [35], however, that, under certain assumptions on the nature of the X , the two states could be indeed reconciled with one another. In particular, it was argued in Ref. [35] that the X , as a virtual state in the $D\bar{D}^*$ system, can reproduce both sets of data, for the $DD\pi$ and $\rho J/\psi$ channels, whereas in the latter case one deals with a threshold cusp. Parameters of the model were tuned to fit all the data on the resonance width and branching ratios. These results of Ref. [35] appear to be in a good agreement with the findings of Refs. [21,25]. The analysis of Ref. [35] is improved in Ref. [36] where additional non- $D\bar{D}^*$ modes of the X were taken into account and the admixture of the genuine $c\bar{c}$ charmonium in the X wave function was estimated.

Recently Belle Collaboration announced a new analysis for the $D^{*0}\bar{D}^0$ case [37]. The new data on the $D^{*0} \rightarrow D^0\pi^0$

¹An obvious shorthand notation is used here and in what follows: $D\bar{D}^* \equiv \frac{1}{\sqrt{2}}(D\bar{D}^* + \bar{D}D^*)$.

and $D^{*0} \rightarrow D^0 \gamma$ channels were fitted both with the simple Breit–Wigner line–shape form and with the Flatté formula. As a result, a lower position of the peak,

$$M_X = 3872.6_{-0.4}^{+0.5} \pm 0.4 \text{ MeV}, \quad (15)$$

was obtained than the one reported before—see Eq. (13). The corresponding branching ratio was measured to be

$$\text{Br}(B^+ \rightarrow K^+ X(D^{*0} \bar{D}^0)) = (0.73 \pm 0.17 \pm 0.13) \times 10^{-4}. \quad (16)$$

These new data are analyzed in Ref. [38] using the technique very close to that of Ref. [35], and the conclusion is made that the X is a $2^3P_1 \bar{c}c$ state strongly distorted by couple channel effects.

In this paper we present an updated Flatté analysis, with the new data on the $D^0 \bar{D}^{*0}$ mode [37] and on the $\gamma \psi'$ mode [8] included. In particular, we address the question of a possible χ'_{c1} charmonium admixture in the wave function of the $X(3872)$. The strategy employed in this paper, differs significantly from the one of Ref. [35], where a model-blind Flatté analysis was performed. Here we assume a mechanism for the X production via the charmonium component.

The paper is organized as follows. In Sec. II we give necessary details of the Flatté parametrization for a near-threshold resonance and apply this technique to the case of the $X(3872)$. We analyze the data in Sec. III, and comment on the effect of the D^{*0} finite width in Sec. IV. We conclude and discuss the results in Sec. V.

II. FLATTÉ PARAMETRIZATION

In this Section we introduce a Flatté-like parametrization of the near–threshold observables related to the $X(3872)$ state. Let us define the energy E relative to the neutral $D^0 \bar{D}^{*0}$ threshold [see Eq. (11)]. Then the relevant energy range is approximately $-10 \text{ MeV} \lesssim E \lesssim 10 \text{ MeV}$ which covers both the three-body $D^0 \bar{D}^0 \pi^0$ threshold at $E_{D^0 \bar{D}^0 \pi^0} \approx -7 \text{ MeV}$ and the charged $D^+ \bar{D}^{*-}$ threshold at $E_{D^+ \bar{D}^{*-}} \equiv \delta \approx 7.6 \text{ MeV}$. A natural generalization of the standard Flatté parametrization for the near–threshold resonance [39] of the $D^0 \bar{D}^{*0}$ scattering amplitude reads

$$F(E) = -\frac{1}{2k_1} \frac{g_1 k_1}{D(E)}, \quad (17)$$

with

$$D(E) = \begin{cases} E - E_f - \frac{g_1 k_1}{2} - \frac{g_2 k_2}{2} + i \frac{\Gamma(E)}{2}, & E < 0 \\ E - E_f - \frac{g_2 k_2}{2} + i \left(\frac{g_1 k_1}{2} + \frac{\Gamma(E)}{2} \right), & 0 < E < \delta \\ E - E_f + i \left(\frac{g_1 k_1}{2} + \frac{g_2 k_2}{2} + \frac{\Gamma(E)}{2} \right), & E > \delta \end{cases} \quad (18)$$

and

$$k_1 = \sqrt{2\mu_1 E}, \quad \kappa_1 = \sqrt{-2\mu_1 E}, \\ k_2 = \sqrt{2\mu_2(E - \delta)}, \quad \kappa_2 = \sqrt{2\mu_2(\delta - E)}.$$

Here μ_1 and μ_2 are the reduced masses in the $D^0 \bar{D}^{*0}$ and $D^+ \bar{D}^{*-}$ channels, respectively. Assuming isospin conservation we set $g_1 = g_2 = g$.

The term $i\Gamma(E)/2$ in Eq. (18) accounts for non- $D\bar{D}^*$ modes:

$$\Gamma(E) = \Gamma_{\pi^+ \pi^- J/\psi}(E) + \Gamma_{\pi^+ \pi^- \pi^0 J/\psi}(E) + \Gamma_0, \quad (19)$$

where we single out the first two modes because of their explicit energy dependence:

$$\Gamma_{\pi^+ \pi^- J/\psi}(E) = f_\rho \int_{2m_\pi}^{M-m_{J/\psi}} \frac{dm}{2\pi} \frac{q(m)\Gamma_\rho}{(m - m_\rho)^2 + \Gamma_\rho^2/4}, \quad (20)$$

$$\Gamma_{\pi^+ \pi^- \pi^0 J/\psi}(E) = f_\omega \int_{3m_\pi}^{M-m_{J/\psi}} \frac{dm}{2\pi} \frac{q(m)\Gamma_\omega}{(m - m_\omega)^2 + \Gamma_\omega^2/4}, \quad (21)$$

with f_ρ and f_ω being effective couplings and

$$q(m) = \sqrt{\frac{(M^2 - (m + m_{J/\psi})^2)(M^2 - (m - m_{J/\psi})^2)}{4M^2}} \quad (22)$$

being the center-of-mass di-pion/tri-pion momentum ($M = E + M(D^0 \bar{D}^{*0})$).

Now, if we assume the short-ranged dynamics of the weak $B \rightarrow K$ transition to be absorbed into the coefficient \mathcal{B} , then the differential rates of interest in the Flatté approximation read:

$$\frac{d\text{Br}(B \rightarrow K D^0 \bar{D}^{*0})}{dE} = \mathcal{B} \frac{1}{2\pi} \frac{g k_1}{|D(E)|^2}, \quad (23)$$

$$\frac{d\text{Br}(B \rightarrow K \pi^+ \pi^- J/\psi)}{dE} = \mathcal{B} \frac{1}{2\pi} \frac{\Gamma_{\pi^+ \pi^- J/\psi}(E)}{|D(E)|^2}, \quad (24)$$

and

$$\frac{d\text{Br}(B \rightarrow K \pi^+ \pi^- \pi^0 J/\psi)}{dE} = \mathcal{B} \frac{1}{2\pi} \frac{\Gamma_{\pi^+ \pi^- \pi^0 J/\psi}(E)}{|D(E)|^2}. \quad (25)$$

Obviously, the rate (23) is defined for $E > 0$ only, while the rates (24) and (25) are defined both above and below the $D^0 \bar{D}^{*0}$ threshold. Strictly speaking, one is to take into account a finite width of the D^* , which is very small however. Indeed, the total width of the $D^{*\pm}$ -meson is measured to be $96 \pm 22 \text{ keV}$ [12]. There are no data on the D^{*0} width, but one can estimate the total width of the D^{*0} from the data [12] on charged $D^{*\pm}$ to be about 63 keV , which gives $\Gamma(D^{*0} \rightarrow D^0 \pi^0) = 42 \text{ keV}$. If, nevertheless, the finite width of the D^* is taken into account, the rate (23)

continues to the region $E < 0$ and interference effects are possible in the final state, as described in Ref. [40]. We shall discuss this in some detail below though, at the moment, we follow Refs. [35,36] and neglect the D^* width.

Now, in order to proceed to the branching ratio to the $DD\pi$ final state, one is to take into account the branching fractions of the D^{*0} [12]:

$$\text{Br}(D^{*0} \rightarrow D^0 \pi^0) = (61.9 \pm 2.9)\%, \quad (26)$$

$$\text{Br}(D^{*0} \rightarrow D^0 \gamma) = (38.1 \pm 2.9)\%, \quad (27)$$

so that

$$\frac{d\text{Br}(B \rightarrow KD^0 \bar{D}^0 \pi^0)}{dE} = 0.62 \mathcal{B} \frac{1}{2\pi} \frac{gk_1}{|D(E)|^2}. \quad (28)$$

Analogously we have for the $D^0 \bar{D}^0 \gamma$ differential rate:

$$\frac{d\text{Br}(B \rightarrow KD^0 \bar{D}^0 \gamma)}{dE} = 0.38 \mathcal{B} \frac{1}{2\pi} \frac{gk_1}{|D(E)|^2}. \quad (29)$$

With the Flatté parametrization introduced above, one can make use of the method suggested in Ref. [41] to estimate the admixture of a bare χ'_{c1} state in the wave function of the X . Indeed, in the context of $c\bar{c}$ - $D\bar{D}^*$ coupled-channel model the quantities entering the Flatté-type expressions for differential rates acquire clear physical meaning. Namely, the coefficient \mathcal{B} can be viewed as the branching fraction $B \rightarrow K\chi'_{c1}$, g is the bare $\chi'_{c1} D\bar{D}^*$ coupling constant, and Γ_0 is the bare total width of the χ'_{c1} level. Moreover, as shown in Ref. [41], in the Flatté limit, the probability $w(E)$ to find the bare state in the wave function of a physical state can be expressed in terms of Flatté parameters as

$$w(E) = \frac{1}{2\pi |D(E)|^2} (gk_1 \Theta(E) + gk_2 \Theta(E - \delta) + \Gamma(E)). \quad (30)$$

The admixture W of the χ'_{c1} charmonium in the resonance wave function can be defined as

$$W = \int_{E_{\min}}^{E_{\max}} w(E) dE, \quad (31)$$

where the integral is taken over the near-threshold region. As was discussed before, we choose it to be from -10 MeV to $+10$ MeV.

III. DATA ANALYSIS

A. Essentials and constraints

In this chapter we analyze the existing data using the Flatté approach described above. Our aim is to estimate the admixture of the charmonium component of the X wave function and to identify the nature of the residual, dynamically generated part of its wave function. In particular, we shall answer the question as to whether the existing experi-

mental data are compatible with the bound state or virtual state in the $D^0 D^{*0}$ system.

Let us comment briefly on the difference between the bound/virtual state situations.

In the Flatté approximation the inelastic differential rate is

$$\mathcal{B} \frac{1}{2\pi} \frac{\Gamma(E)}{|D(E)|^2}. \quad (32)$$

One can see easily that the behavior of the inelastic rate below threshold depends strongly on whether there is a zero in the real part of the denominator $D(E)$ below threshold. Indeed, if $D(E_{\text{bound}}) = 0$ for some $E_{\text{bound}} < 0$ then, for $\Gamma(E) \rightarrow 0$, the inelastic rate (32) does not vanish, but becomes proportional to a δ -function:

$$\mathcal{B} \left(\frac{\partial D(E)}{\partial E} \Big|_{E=E_B} \right)^{-1} \delta(E - E_{\text{bound}}). \quad (33)$$

We end up therefore with a real bound state, which is not coupled to inelastic channels.

On the contrary, if there is no such zero (virtual state case), the rate (32) vanishes as $\Gamma(E) \rightarrow 0$, while the $D^0 \bar{D}^{*0}$ rate does not vanish in this limit.

Consider the case of $\Gamma_0 = 0$ first. In this case, in order to distinguish between these two scenarios (bound state versus virtual state) one is, as was argued in [24,35], to check the ratio

$$\frac{\text{Br}(X \rightarrow D^0 \bar{D}^0 \pi^0)}{\text{Br}(X \rightarrow \pi^+ \pi^- J/\psi)}, \quad (34)$$

which varies from quite small (and hardly resolvable experimentally against the background) values, for the bound-state scenario, up to values of order ten (in Ref. [35] this ratio was calculated to be 9.9) for the virtual state. It follows from the data quoted in Eqs. (6) and (14) that the ratio (34) is indeed large ($\approx 10 \div 15$), which seems to indicate the virtual-state nature of the X . However, the above consideration was based on the assumption that, once produced, the X state can only decay through one of the three channels: $D^0 \bar{D}^0 \pi$ or $\rho J/\psi$ and $\omega J/\psi$ (the $\gamma J/\psi$ mode is small, and was neglected). Nowadays, a new $\gamma \psi'$ mode is observed. Moreover, if it is presumably due to $c\bar{c}$ bare seed, then extra decay channels typical for charmonium should exist for the X , which are encoded in the extra width $\Gamma_0 \neq 0$. These are annihilation modes (into light hadrons), and $\chi_{c1}(3515) \pi\pi$ (the latter was estimated in Ref. [42] to be of order of a few keV). The total width of the $\chi_{c1}(3515)$ is 0.89 ± 0.05 MeV, and the branching fraction into radiative $\gamma J/\psi$ mode is about 36% [12]. If it were a true guide, then one expects the width of the χ'_{c1} to be about $1 \div 2$ MeV. Quark model prediction [30] yields the value of 1.72 MeV for the total width of the χ'_{c1} . In accordance with predictions (12), radiative modes are not the dominant ones.

Now the ratio (34) should be modified to read:

$$\frac{\text{Br}(X \rightarrow D^0 \bar{D}^0 \pi^0)}{\text{Br}(X \rightarrow \text{non}D^0 \bar{D}^0 \pi^0)} \sim 1, \quad (35)$$

opening the possibility for the X being a bound state.²

Finally, assuming the X to be produced via the χ'_{c1} component of its wave function, one can estimate the coefficient \mathcal{B} . The world average for the $\text{Br}(B^+ \rightarrow K^+ \chi_{c1})$ is [12]

$$\text{Br}(B^+ \rightarrow K^+ \chi_{c1}) = (5.1 \pm 0.5) \times 10^{-4}, \quad (36)$$

and it is known [12] that J/ψ and ψ' are produced in the $B \rightarrow K$ decays with comparable branching fractions:

$$\text{Br}(B^+ \rightarrow K^+ J/\psi) = (10.22 \pm 0.35) \times 10^{-4},$$

$$\text{Br}(B^+ \rightarrow K^+ \psi') = (6.48 \pm 0.35) \times 10^{-4}.$$

Then it is reasonable to assume that the χ'_{c1} is produced in the $B \rightarrow K$ decays with the rate comparable to (36). There exists a quark model prediction [44] $\text{Br}(B \rightarrow K \chi'_{c1}) = 2 \times 10^{-4}$. However, the model used in Ref. [44] underestimates the rate (36) more than 2 times.

As was mentioned before, the admixture of the genuine charmonium in the X wave function is given by the quantity W defined in Eqs. (30) and (31).

Therefore, our analysis strategy is to approximate the existing experimental data on the $D\bar{D}^*$ and $\pi^+ \pi^- J/\psi$ decay modes of the X with the Flatté formulas and

- (i) to find the admixture of the χ'_{1c} charmonium in the X wave function by evaluating the integral (31) of the spectral density (30) over the near-threshold region;
- (ii) to compute the scattering length for the $D\bar{D}^*$ system and thus to make a conclusion concerning its virtual/bound-state nature;
- (iii) to investigate the effect of the finite-width Γ_0 .

The data on the $D\bar{D}^*$ and $\pi^+ \pi^- J/\psi$ modes are analyzed under the following constraints:

- (i) $\text{Br}(B \rightarrow K \chi'_{c1}) = \mathcal{B} = (3 \div 6) \times 10^{-4}$, with the preference to lower values [see Eq. (36) and the discussion following it];
- (ii) $\text{Br}(B \rightarrow KX) = \mathcal{B}W < 3.2 \times 10^{-4}$ [the limit imposed by the *BABAR* data [9], see Eq. (9)];
- (iii) $\Gamma_0 = 1 \div 2$ MeV (as discussed above).

Throughout this paper we deal only with the data on the charged B -meson decays, as the uncertainties in the data on the neutral mode remain large. Belle Collaboration presents the data on the $D^0 \bar{D}^0 \pi^0$ and $D^0 \bar{D}^0 \gamma$ modes separately, and we analyze only the former mode (again due to larger uncertainties in the $D^0 \bar{D}^0 \gamma$ mode). *BABAR* data presented are for all $D^0 \bar{D}^{*0}$ modes, so we consider these data.

²The idea that, including an extra width, one can fit the data on the $X(3872)$ both with virtual and bound state was first presented in Ref. [43].

B. Belle collaboration data

As it was mentioned in the introductory part, recently Belle Collaboration presented a new analysis for the $\pi^+ \pi^- J/\psi$, $D\bar{D}\pi$, and $D\bar{D}\gamma$ decay modes of the X [7,37]. These new data differ significantly from the old ones. The peak in the $\pi^+ \pi^- J/\psi$ mass distribution is shifted to the left, making the virtual state/cusp scenario advocated in Ref. [35] less plausible. However, as the ratio (34) remains large, extra non- $D\bar{D}\pi$ modes are needed in order to arrive at the bound-state solution, as it follows from Eq. (35) and will be shown below.

In order to translate the differential rates into number-of-events distributions, we notice that there are 131 signal events in the Belle data for the $\pi^+ \pi^- J/\psi$ channel [7], which corresponds to the branching fraction of about 8.1×10^{-6} ; the bin size is 2.5 MeV. Then

$$N_{\text{Belle}}^{\pi\pi J/\psi}(E) = 2.5 [\text{MeV}] \left(\frac{131}{8.3 \cdot 10^{-6}} \right) \times \frac{d\text{Br}(B \rightarrow K \pi^+ \pi^- J/\psi)}{dE}. \quad (37)$$

Similarly, for the $D^0 \bar{D}^0 \pi^0$ mode, the Belle Collaboration states to have 48.3 signal events in the charged mode [37], which corresponds to the branching fraction of about 0.73×10^{-4} ; the bin size is 2 MeV. Thus the number-of-events distributions is calculated as

$$N_{\text{Belle}}^{D^0 \bar{D}^0 \pi^0}(E) = 2.0 [\text{MeV}] \left(\frac{48.3}{0.73 \cdot 10^{-4}} \right) \times \frac{d\text{Br}(B \rightarrow K D^0 \bar{D}^0 \pi^0)}{dE}. \quad (38)$$

In the latter case, the background function is proportional to the two-body $D^0 \bar{D}^{*0}$ phase space $R_2 \propto \sqrt{E}$, that is the background is considered to be due to the contribution of the $D^0 \bar{D}^{*0}$ and, as such, to interfere with the signal:

$$\frac{d\text{Br}(B \rightarrow K D^0 \bar{D}^0 \pi^0)}{dE} = 0.62 \frac{k_1}{2\pi} \left[\left(\text{Re} \frac{\sqrt{g\mathcal{B}}}{D(E)} + c \cos\phi \right)^2 + \left(\text{Im} \frac{\sqrt{g\mathcal{B}}}{D(E)} + c \sin\phi \right)^2 \right], \quad (39)$$

with the relative phase ϕ and c being fitting constants.

Finally, the resolution functions for both reactions are taken in the form of Gaussians with the fixed resolution scale being 3 MeV, for the $\pi^+ \pi^- J/\psi$ channel, and with the variable mass-dependent resolution function $\sigma(m) = a\sqrt{m - m_0}$, with $a = 0.172$ MeV^{1/2} and $m_0 = M(D\bar{D}^*)$ [37].

The Belle data on the $D^0 \bar{D}^0 \pi^0$ mode [37] can be equally well described by both the virtual state and the bound state in the $D\bar{D}^*$ system (set 1 and sets 2, 3 in Table I and plots in Figs. 1 and 2, respectively). For set 1, the width Γ_0 mimics the $\gamma\psi'$ decay channel and is fixed through the condition that $\text{Br}(\gamma\psi') \simeq \text{Br}(\pi\pi J/\psi)$. However, the description of

TABLE I. The sets of the Flatté parameters for the Belle data from Refs. [7,37].

Set	Γ_0 , MeV	g	E_f , MeV	f_ρ	f_ω	$\mathcal{B} \times 10^4$	ϕ	W	$\mathcal{B}W \times 10^4$	a , fm
1	1.1	0.3	-12.8	0.00770	0.04070	2.7	180°	0.19	0.5	-5.0 - i 1.3
2	1.0	0.137	-12.3	0.00047	0.00271	4.3	153°	0.43	1.9	3.5 - i 1.0
3	2.0	0.091	-7.8	0.00090	0.00523	3.7	152°	0.52	1.9	3.3 - i 1.7

the Belle data on the $\pi^+ \pi^- J/\psi$ mode is remarkably poor for this set—see Fig. 1. Besides that, the radiative width of about 1 MeV seems to be suspiciously large and, in any case, is not compatible with χ'_{c1} assumption.

We find therefore that a decent description of the Belle data on the $\pi^+ \pi^- J/\psi$ mode is only possible with a bound state (see sets 2 and 3 in Table I and in Fig. 2). Furthermore, because of a considerable contribution of the finite-width Γ_0 to the spectral density $w(E)$, its integral over the near-threshold region appears to be rather large (see Table I) which indicates a significant admixture of the genuine charmonium state in the X wave function.

It is instructive to study the behavior of the spectral density for the bound-state case in more detail. It is plotted in Fig. 3, where the contribution of non- $D\bar{D}^*$ modes is also shown which peaks at the position of the bound-state mass. Using the relation between the Flatté parameters and the effective range parameters established in Ref. [41], it is straightforward to demonstrate that, in the limit of vanishing inelasticity, the spectral density below the $D^0\bar{D}^{*0}$ threshold becomes, similarly to the inelastic rate (32) proportional to a δ -function,

$$w(E) \rightarrow Z\delta(E - E_{\text{bound}}), \quad E < 0, \quad (40)$$

with the coefficient Z being nothing but the famous Z -factor which was introduced by Weinberg in Ref. [45] and which defines the probability to find a bare state in the wave function of a physical bound state with the binding

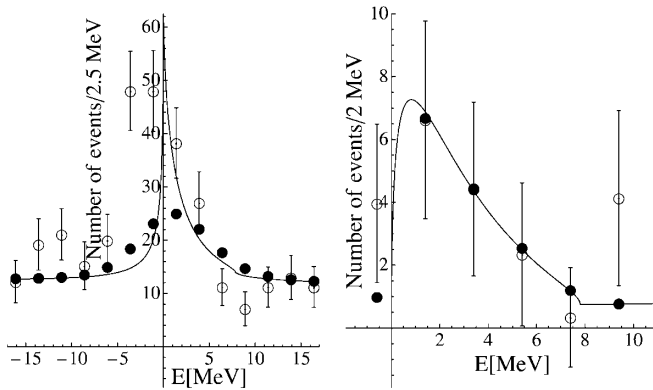


FIG. 1. Differential rates for the $\pi^+ \pi^- J/\psi$ channel (left plot) and $D^0\bar{D}^0\pi^0$ channel (right plot) [see Eqs. (37) and (38), respectively] with the parameters given by set 1 (see Table I). The distributions integrated over the bins, with resolution function taken into account, are shown as filled dots, experimental data (see Refs. [7,37]) are given as open dots with error bars.

energy E_{bound} . So it is reasonable to define an integral over the near-threshold region:

$$Z = \int_{E_{\text{min}}}^{E_{\text{max}}} w_{\text{inel}}(E) dE, \quad (41)$$

with

$$w_{\text{inel}}(E) = \frac{1}{2\pi|D(E)|^2} \Gamma(E). \quad (42)$$

Then the factor Z can be viewed as the Z -factor of our bound states smeared due to the presence of the inelasticity and it takes the values:

$$Z = 0.31 \text{ (set2)}, \quad Z = 0.37 \text{ (set3)}. \quad (43)$$

The values of the branchings $\text{Br}(B \rightarrow K\chi'_{c1}) = \mathcal{B}$ and $\text{Br}(B \rightarrow KX) = \mathcal{B}W$, as given in Table I, agree with the constraints imposed on them by experimental data and quoted in the beginning of this section. The radiative decay width appears to be in a reasonable agreement with quark

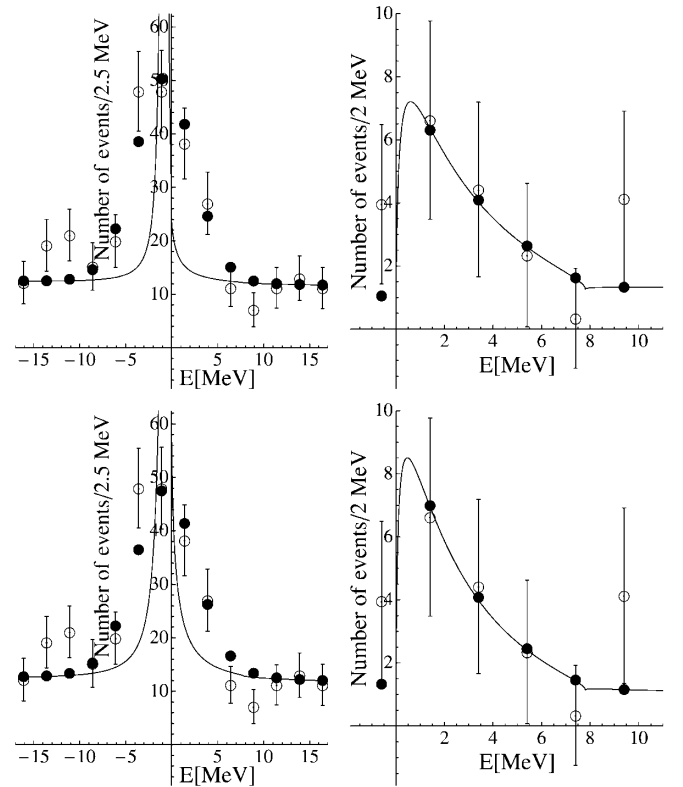


FIG. 2. The same as in Fig. 1 but for set 2 (upper plots) and set 3 (lower plots).

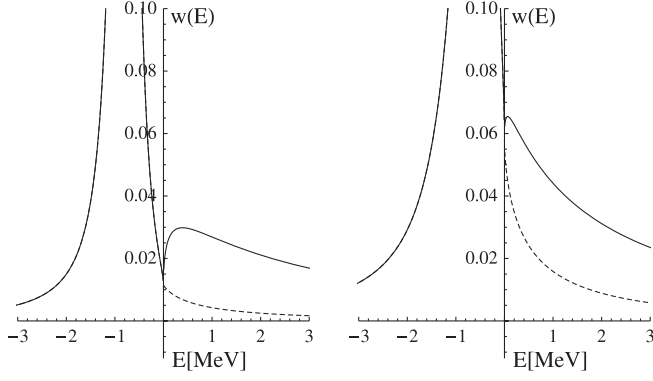


FIG. 3. Spectral density for set 2 (first plot) and set 3 (second plot). The full spectral density $w(E)$ is plotted with the solid line, the contribution $w_{\text{inel}}(E)$ of the non- $D\bar{D}^*$ channels to the spectral density is shown with the dashed line. The functions $w(E)$ and $w_{\text{inel}}(E)$ coincide below threshold.

model estimates (7):

$$\begin{aligned}\Gamma(\gamma\psi') &= 60 \text{ keV (set2),} \\ \Gamma(\gamma\psi') &= 110 \text{ keV (set3).}\end{aligned}\quad (44)$$

Therefore, one can make the conclusion that the new Belle data favor the $X(3872)$ to be a mixture of a genuine charmonium and a dynamically generated moleculelike state which appears to be a bound state of the $D^0\bar{D}^{*0}$ system.

C. BABAR collaboration data

In the data analysis procedure, similarly to the Belle data case, the formulas for the number-of-events distributions were taken to be:

$$\begin{aligned}N_{\text{BaBar}}^{\pi\pi J/\psi}(E) &= 5 \text{ [MeV]} \left(\frac{93.4}{8.4 \times 10^{-6}} \right) \\ &\times \frac{d\text{Br}(B \rightarrow K\pi^+\pi^-J/\psi)}{dE},\end{aligned}\quad (45)$$

for the $\pi^+\pi^-J/\psi$ mode [bin size is 5 MeV, the number of events is 93.4, and $\text{Br}(B \rightarrow K\pi^+\pi^-J/\psi) = 8.4 \times 10^{-6}$ —see Ref. [6]], and

$$\begin{aligned}N_{\text{BaBar}}^{D^0\bar{D}^{*0}}(E) &= 2.0 \text{ [MeV]} \left(\frac{33.1}{1.67 \times 10^{-4}} \right) \\ &\times \frac{d\text{Br}(B \rightarrow KD^0\bar{D}^{*0})}{dE},\end{aligned}\quad (46)$$

for the $D^0\bar{D}^{*0}$ mode [the bin size is 2 MeV, number of events is 33.1, and $\text{Br}(B \rightarrow KD^0\bar{D}^{*0}) = 1.67 \cdot 10^{-4}$; all $D^0\bar{D}^{*0}$ modes are included—see Ref. [34]]. The signal-background interference is taken into account in the same manner as for the Belle data—see Eq. (40), with the factor 0.62 omitted.

The resolution function for the $\pi^+\pi^-J/\psi$ channel is taken in the form of a Gaussian with the fixed resolution scale being 4.38 MeV [6]. As to the $D\bar{D}^*$ resolution, it is described by the BABAR Collaboration as a very complicated function, and it is not available in public domain. In the present analysis we take, with corresponding reservations, this resolution also to be Gaussian, with the resolution scale of 1 MeV.

The BABAR $D^0\bar{D}^{*0}$ data [34] are very similar to the old Belle ones [33], while the $\pi^+\pi^-J/\psi$ peak in Ref. [6] is moved a bit to the left in comparison with the old BABAR data on the same reaction, and the peak width has decreased around 25% due to a better resolution. One expects therefore, that the $D^0\bar{D}^{*0}$ data are better described as a virtual state, while the $\pi^+\pi^-J/\psi$ data complies better with the bound state. Correspondingly, we employ two different analysis strategies. First, we reconcile the $\pi^+\pi^-J/\psi$ and $D^0\bar{D}^{*0}$ peaks with each other, as it was done in [35,36] (sets 4 and 5). The second strategy is to find the best overall description of the both data sets (sets 6 and 7). The parameters for these sets are given in Table II, and the differential rates are shown in Figs. 4 and 5.

The reconciling procedure yields a virtual state, similar to the one found in Refs. [35,36]. The admixture of the charmonium is not large for these sets and, again, the radiative decay width $\Gamma(\gamma\psi')$ seems to be too large for the charmonium assignment:

$$\begin{aligned}\Gamma(\gamma\psi') &= 800 \text{ keV (set4),} \\ \Gamma(\gamma\psi') &= 500 \text{ keV (set5).}\end{aligned}\quad (47)$$

The overall description of the data seems to be not too bad, as the present resolution cannot confirm or rule out the $\pi^+\pi^-J/\psi$ cusp scenario.

Solutions 6 and 7, obtained from the overall fit to the BABAR data, clearly prefer the bound-state, similarly to the ones given by sets 2 and 3 for the Belle data. The charmonium admixture is even larger than for the Belle version (see Table II), and the $\Gamma(\gamma\psi')$ width,

TABLE II. The sets of the Flatté parameters for the BABAR data from Refs. [6,34].

Set	Γ_0 , MeV	g	E_f , MeV	f_ρ	f_ω	$\mathcal{B} \times 10^4$	ϕ	W	$\mathcal{B}W \times 10^4$	a , fm
4	1.0	0.225	-9.7	0.0065	0.0360	3.9	113°	0.24	1.8	-4.9 - i 1.6
5	2.0	0.145	-6.0	0.0040	0.0230	3.6	109°	0.34	0.8	-3.9 - i 2
6	1.0	0.080	-8.4	0.0002	0.0010	5.7	0°	0.58	3.3	2.2 - i 0.3
7	2.0	0.090	-9.0	0.0005	0.0029	5.5	0°	0.53	2.9	3.3 - i 0.7

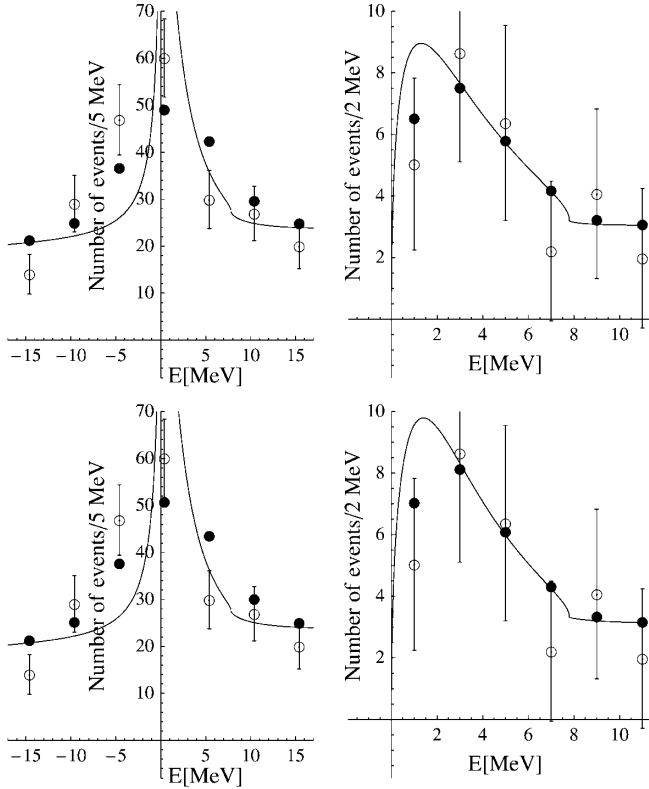


FIG. 4. Differential rates for the $\pi^+\pi^-J/\psi$ channel (left plots) and $D^0\bar{D}^{*0}$ channel (right plots) [see Eqs. (45) and (46), respectively] with the parameters given by set 4 (upper plots) and set 5 (lower plots). Parameters from these sets are presented in Table II. The distributions integrated over the bins, with resolution function taken into account, are shown as filled dots, experimental data (see Refs. [6,34]) are given as open dots with error bars.

$$\Gamma(\gamma\psi') = 25 \text{ keV (set6)}, \quad \Gamma(\gamma\psi') = 60 \text{ keV (set7)}, \quad (48)$$

is a bit small as compared to the estimates (7). The $\pi^+\pi^-J/\psi$ data are described better than in the virtual-state version, while the description of the $D^0\bar{D}^{*0}$ data is rather poor (it remains an open question either it is genuine, or is due to our ill-starred guess on the *BABAR* $D^0\bar{D}^{*0}$ resolution function).

Therefore, we find that the *BABAR* data are more compatible with the assumption of the $X(3872)$ being a virtual state of a dynamical nature. As to the charmonium admixture, we can only state that it is small. Indeed, as shown in Ref. [41], in the case of small values of W , the model-independent Flatté analysis does not allow one to draw any conclusions on the binding mechanism, that is to distinguish between t -channel meson exchange forces or short-ranged s -channel forces due to coupling of bare states to the hadronic channel. One can only state that the properties of the resonance are given mainly by the hadronic contin-

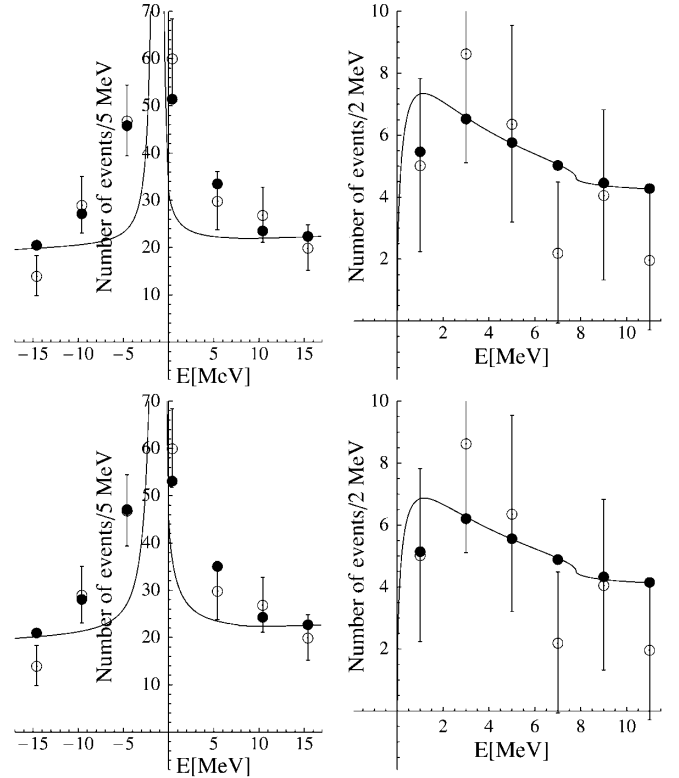


FIG. 5. The same as in Fig. 4 but for set 6 (upper plots) and set 7 (lower plots).

uum contribution, and the state is mostly of a dynamical (molecular) nature.

We conclude this section with the comment on the paper [38], where the Flatté fits were performed similar to ours, and the pole structure of the Flatté amplitude was studied. Conclusions on the nature of the X were drawn in Ref. [38] based on the pole-counting procedure developed in Ref. [46]: two near-threshold poles correspond to a large admixture of a bare state in the resonance wave function, while a single near-threshold pole indicates a dynamical nature of the resonance. Strictly speaking, the Riemann surface for the X case is much more complicated than the one assumed in Ref. [38], due to the presence of many-body cuts (caused by the $\pi^+\pi^-J/\psi$ and $\pi^+\pi^-\pi^0J/\psi$ modes). However, the pole-counting procedure should yield, qualitatively, the same result as a more rigorous method based on the spectral density calculations employed here, which allows, *inter alia*, to estimate quantitatively the bare state admixture (for more details on the interrelation between the pole-counting and spectral density behavior see Ref. [41]). For the fits with reasonably small values of the factor \mathcal{B} two near-threshold poles were found in Ref. [38], signalling a large admixture of the genuine charmonium, similarly to our Belle parameter sets. Note, however, that the fits presented in Ref. [38] are the overall ones: the Belle and *BABAR* data were fitted simultaneously. As a result, rather poor description of the

$BABAR D^0 \bar{D}^{*0}$ data was obtained, reflecting incompatibility of the new Belle and $BABAR$ data.

IV. COMMENT ON THE D^* FINITE WIDTH

The possibility of the bound-state solution brings on board one more important question. Namely, in the present analysis, the D^{*0} -meson was assumed to be stable. As argued in Ref. [35], account for a small finite width of the D^{*0} does not change the $D^0 \bar{D}^{*0}$ line-shape in the case of the virtual state while, for a bound state, the effects of the finite width could be pronounced, as shown in Ref. [47]. A refined treatment of the finite width is in progress now [48], while here we estimate these effects using a simple ansatz suggested in Ref. [49] and reinvented in Ref. [47]. The recipe is to make the following replacement in the expressions for the $D^0 \bar{D}^{*0}$ momentum entering the formulas for differential rates:

$$\Theta(E)k_1(E) \rightarrow \sqrt{\mu_1} \sqrt{\sqrt{E^2 + \Gamma_*^2/4} + E}, \quad (49)$$

and

$$\Theta(-E)\kappa_1(E) \rightarrow \sqrt{\mu_1} \sqrt{\sqrt{E^2 + \Gamma_*^2/4} - E}, \quad (50)$$

where Γ_* is the width of the D^{*0} -meson. It can be shown [48] that these formulas are valid if the resonance is well-separated from the three-body threshold (the $D^0 \bar{D}^{*0} \pi^0$ threshold in our case), and the zero-width limit is readily reproduced as $\Gamma_* \rightarrow 0$.

To access the role of the finite D^{*0} width we evaluate the $D^0 \bar{D}^{*0}$ differential rates, with $\Gamma_* = 63$ keV, for the sets 2 and 3 (bound-state scenario for the Belle data) and for the sets 4 and 5 (virtual-state scenario for the $BABAR$ data) and plot them, together with the zero-width rates, in Fig. 6. In particular, in this figure, we show our theoretical curves given by expressions (23), with the replacement (49) and (50), and with the Flatté parameters from the corresponding tables, without signal-background interference and not smeared with the resolution functions.

As seen from Fig. 6, the virtual-state solutions are not affected by the finite D^{*0} width at all (lower plots). In the meantime, the bound-state excitation curves are not affected either, in the above-threshold region, and a non-negligible $D^0 \bar{D}^{*0} \pi^0$ peak is developed around the bound-state mass position (upper plots).

The bound-state peak resides at about -0.75 MeV for set 2 and at about -0.5 MeV for set 3, so the only effect expected is an increase of the number of events in the first near-threshold bin. Indeed, for the Belle bound-state solutions, we have calculated the ratio \tilde{N}_i/N_i of the number of events in the first ($i = 1$) and second ($i = 2$) nonempty Belle bins, with (\tilde{N}_i) and without (N_i) inclusion of the finite width:

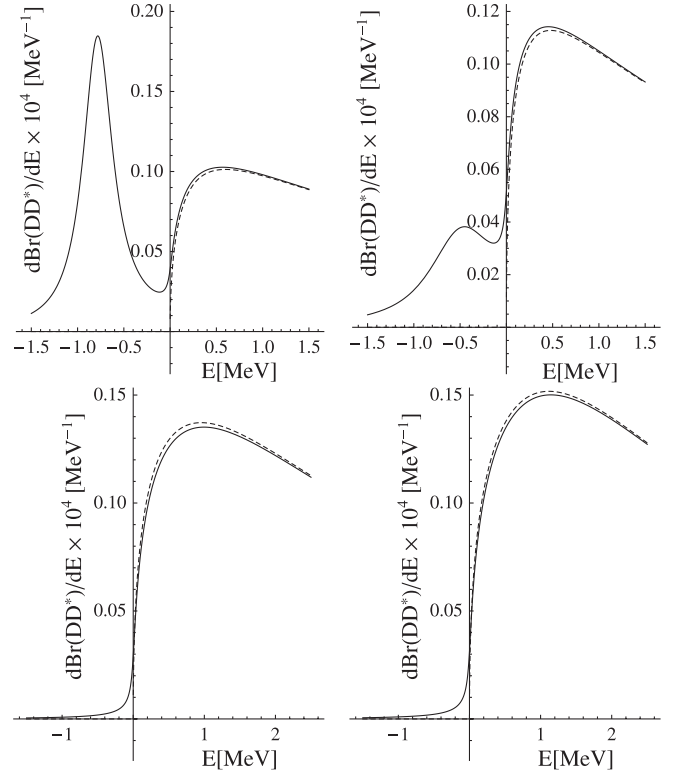


FIG. 6. Upper plots: the differential rates for the $D^0 \bar{D}^{*0}$ channel given by the Flatté formula with the finite-width Γ_* included (solid lines) and with the zero width (dashed lines) for parameters sets 2 (left) and 3 (right). Lower plots: the same as in the upper plots but for parameters sets 4 and 5.

$$\begin{aligned} \tilde{N}_1/N_1 &= 4.31, & \tilde{N}_2/N_2 &= 1.01 \text{ (set2),} \\ \tilde{N}_1/N_1 &= 1.99, & \tilde{N}_2/N_2 &= 1.00 \text{ (set3),} \end{aligned}$$

where the ratios above are calculated without resolution and signal-background interference. Clearly, a large value of the ratio \tilde{N}_1/N_1 does not cause problems, as Belle bound-state solutions underestimate the number of events in the lowest bin only (see Fig. 2), and the number of events in higher bins is not affected by the finite-width effect.

Thus a considerable number of the $D^0 \bar{D}^{*0}$ events is to appear below the nominal $D^0 \bar{D}^{*0}$ threshold in the bound-state case. In the meantime, the present experimental situation does not allow one to identify the bound-state peak. This must be attributed to the peculiarities of the data analysis: both $BABAR$ and Belle Collaborations assume that the $D^0 \bar{D}^{*0} \pi^0$ events come from the $D^0 \bar{D}^{*0}$, distorting in such a way the kinematics of the below-threshold events and feeding artificially the above-threshold region at the expense of the below-threshold one.

In a quite recent paper [50] the $D^0 \bar{D}^{*0} \pi^0$ distributions were obtained with the recipe (49) and (50), and, in order to describe the $D^0 \bar{D}^{*0}$ data, the above-mentioned kinematical distortion was corrected with some feedback from data processing arrangements. As a result, a nice description

of the $D^0\bar{D}^{*0}$ Belle data was obtained with a bound-state solution (the description of the *BABAR* data is rather poor in Ref. [50], quite similar to our *BABAR* bound-state solutions 6 and 7). Notice, however, that the solutions of Ref. [50] differ from ours in several respects. First, the data on $\pi^+\pi^-J/\psi$ and $D^0\bar{D}^{*0}$ modes are analyzed separately in Ref. [50], so that it remains unclear whether the presented solutions provide a tolerable overall fit. Second, there is no extra width Γ_0 in the fits describing the $D^0\bar{D}^{*0}$ mode (in fact, there is no inelasticity at all in the best fits for the $D^0\bar{D}^{*0}$ data). Besides that, the scattering length approximation for the $D^0\bar{D}^{*0}$ scattering amplitude is employed in Ref. [50], which is not adequate for our solutions.

Finally, related to the question of the finite D^{*0} width is the problem of the interference in the decay chains $X \rightarrow D^0\bar{D}^{*0} \rightarrow D^0\bar{D}^0\pi^0$ and $X \rightarrow \bar{D}^0D^{*0} \rightarrow D^0\bar{D}^0\pi^0$. According to the estimates made in Ref. [40], the interference effects could enhance the below-threshold $D^0\bar{D}^0\pi^0$ rate up to two times, however the effect is much more moderate above threshold [48]. As to the $X \rightarrow D^0\bar{D}^{*0} \rightarrow D^0\bar{D}^0\gamma$ and $X \rightarrow \bar{D}^0D^{*0} \rightarrow D^0\bar{D}^0\gamma$ decay chains, these are shown to interfere destructively [40]. The proper account for the interference cannot be done in the over-simplified framework presented here, as this effect is to be included in the coupled-channel scheme from the very beginning [48].

V. DISCUSSION AND OUTLOOK

The present analysis was prompted mainly by two recent experimental results: the discovery of the new $\Gamma(\gamma\psi')$ mode of the $X(3872)$ [8] and the new Belle data [37] on the $D^0\bar{D}^{*0}$ mode. We have arrived at conclusions different from the ones of the papers [35,36]. It is instructive to discuss in detail the relation between these new results and the previous ones.

To begin with, the $\Gamma(\gamma\psi')$ mode is to be included in the analysis. As the corresponding rate is comparable to the $\pi^+\pi^-J/\psi$ one, virtual-state solutions yield a very large radiative decay width, about $500 \div 800$ keV which, at present, has no reasonable explanation.

Furthermore, we have demonstrated that the new Belle data on the $D^0\bar{D}^{*0}$ mode are in conflict with the old Belle data [33], as well as with the *BABAR* data on the same mode (up to the resolution issue, as was mentioned before). If the Belle peak at 3872.6 MeV is real, as suggested by the fine resolution and high statistics of the new Belle data, then there is no need anymore to reconcile the $\pi^+\pi^-J/\psi$ and $D\bar{D}^*$ peaks, and the best fit is consistent with the bound-state solution. However, to overcome the problem of the large ratio (34) of the branching fractions, we are forced to include “extra” non- $D\bar{D}^*$ modes, with the radiative width $\Gamma(\gamma\psi')$ being only a small fraction of these “extra” modes. Thus the difference between the present

results and the ones of Ref. [35] is due to the new data as well as the model-dependence allowed here.

The spectral density was calculated for all solutions presented and it appears that, for the bound-state solutions, there is a significant admixture of the bare state in the X wave function. The properties of the bare state delivered by the bound-state solution are in good agreement with the ones of the χ'_{c1} charmonium: the branching fraction in the $B \rightarrow K$ decay, the total width, and the radiative $\gamma\psi'$ width comply well with the charmonium assignment.

We stress that, in this picture, the X is not a *bona fide* charmonium accidentally residing at the $D^0\bar{D}^{*0}$ threshold. Had it been the case, the integral of the spectral density over the resonance region would have been unity while, for our bound-state solutions, it does not exceed 50%. It is rather a resonance attracted to the threshold, a phenomenon advocated in Ref. [43] and described in microscopical models in Refs. [21,22]. In other words, the X is generated dynamically by a strong coupling of the bare χ'_{c1} state to the $D\bar{D}^*$ hadronic channel, with a large admixture of the $D\bar{D}^*$ molecular component.

On the contrary, the virtual-state solution favored by the *BABAR* data points to a rather small (if any) admixture of the bare state in the X wave function, and there is no need to invoke extra modes. This feature, in principle, could discriminate between bound-state and virtual-state solutions. In practice, the annihilation (light hadrons) modes encoded in the quantity Γ_0 are not easily detectable so, in further studies, one is to rely upon improvements in the data on already observed modes.

In particular, a clear signature for a bound-state solution is the below-threshold $D^0\bar{D}^0\pi^0$ peak. Unfortunately, from the experimental point of view, published data are not decisive, mainly due to the kinematical cuts imposed by the assumption on the $D^0(\bar{D}^0)\pi^0$ mode coming from $D^{*0}(\bar{D}^{*0})$ one. In this regard, we urge both experimental collaborations to overcome this and to perform an unbiased analysis.

ACKNOWLEDGMENTS

The authors are grateful to C. Hanhart for collaboration, reading the manuscript, and critical comments, to T. Aushev (Belle Collaboration) and to R. Faccini, M. A. Mazzoni, A. D’Orazio, and V. Poireau (*BABAR* Collaboration) for valuable discussions of the experimental data. This work was supported by the State Corporation of Russian Federation “Rosatom” and by the grants RFFI-09-02-91342-NNIOa, DFG-436 RUS 113/991/0-1(R), NSh-843.2006.2. A.N. would also like to acknowledge the support of the grants RFFI-09-02-00629a, PTDC/FIS/70843/2006-Fisica, and of the nonprofit “Dynasty” foundation and ICFPM.

- [1] S. K. Choi *et al.* (Belle Collaboration), Phys. Rev. Lett. **91**, 262001 (2003).
- [2] K. Abe *et al.* (Belle Collaboration), arXiv:hep-ex/0505037.
- [3] D. Acosta *et al.* (CDF II Collaboration), Phys. Rev. Lett. **93**, 072001 (2004).
- [4] V. M. Abazov *et al.* (D0 Collaboration), Phys. Rev. Lett. **93**, 162002 (2004).
- [5] B. Aubert *et al.* (BABAR Collaboration), Phys. Rev. D **71**, 071103 (2005).
- [6] B. Aubert *et al.* (BABAR Collaboration), Phys. Rev. D **77**, 111101 (2008).
- [7] I. Adachi *et al.* (Belle Collaboration), arXiv:0809.1224.
- [8] B. Aubert *et al.* (BABAR Collaboration), Phys. Rev. Lett. **102**, 132001 (2009).
- [9] B. Aubert *et al.* (BABAR Collaboration), Phys. Rev. D **74**, 011106 (2006).
- [10] T. Kuhr, QWG2008, Nara, Japan, see also the website: <http://www-cdf.fnal.gov/physics/new/bottom/080724.blessed-X-Mass>.
- [11] K. Abe *et al.* (Belle Collaboration), arXiv:hep-ex/0505038; A. Aulencia *et al.* (CDF Collaboration), Phys. Rev. Lett. **96**, 102002 (2006); **98**, 132002 (2007).
- [12] C. Amsler *et al.*, Phys. Lett. B **667**, 1 (2008).
- [13] T. Barnes, S. Godfrey, and E. S. Swanson, Phys. Rev. D **72**, 054026 (2005).
- [14] C. Cawfield *et al.* (CLEO Collaboration), Phys. Rev. Lett. **98**, 092002 (2007).
- [15] M. Suzuki, Phys. Rev. D **72**, 114013 (2005).
- [16] D. Gamermann and E. Oset, Phys. Rev. D **80**, 014003 (2009).
- [17] M. B. Voloshin and L. B. Okun, Pis'ma Zh. Eksp. Teor. Fiz. **23**, 369 (1976) [JETP Lett. **23**, 333 (1976)].
- [18] N. A. Tornqvist, Phys. Rev. Lett. **67**, 556 (1991); Phys. Lett. B **590**, 209 (2004).
- [19] E. S. Swanson, Phys. Lett. B **588**, 189 (2004).
- [20] F. E. Close and P. Page, Phys. Lett. B **578**, 119 (2004); C. Y. Wong, Phys. Rev. C **69**, 055202 (2004); E. Braaten and M. Kusunoki, Phys. Rev. D **69**, 074005 (2004).
- [21] Yu. S. Kalashnikova, Phys. Rev. D **72**, 034010 (2005).
- [22] I. V. Danilkin and Yu. A. Simonov, arXiv:0907.1088.
- [23] E. Braaten and M. Kusunoki, Phys. Rev. D **69**, 074005 (2004).
- [24] E. Braaten and M. Kusunoki, Phys. Rev. D **72**, 014012 (2005).
- [25] D. V. Bugg, Phys. Lett. B **598**, 8 (2004).
- [26] C. E. Thomas and F. E. Close, Phys. Rev. D **78**, 034007 (2008).
- [27] G.-J. Ding, J.-F. Liu, and M.-L. Yan, Phys. Rev. D **79**, 054005 (2009).
- [28] E. Braaten, M. Lu, and J. Lee, Phys. Rev. D **76**, 054010 (2007).
- [29] S. Fleming, M. Kusunoki, T. Mehen, and U. van Kolck, Phys. Rev. D **76**, 034006 (2007).
- [30] T. Barnes and S. Godfrey, Phys. Rev. D **69**, 054008 (2004).
- [31] E. Braaten and M. Kusunoki, Phys. Rev. D **71**, 074005 (2005).
- [32] G. Majumder, <http://belle.kek.jp/belle/talks/ICHEP2006/Majumber.ppt>.
- [33] G. Gokhroo *et al.* (Belle Collaboration), Phys. Rev. Lett. **97**, 162002 (2006).
- [34] B. Aubert *et al.* (BABAR Collaboration), Phys. Rev. D **77**, 011102 (2008).
- [35] C. Hanhart, Yu. S. Kalashnikova, A. E. Kudryavtsev, and A. V. Nefediev, Phys. Rev. D **76**, 034007 (2007).
- [36] Yu. S. Kalashnikova, Proc. Sci., CONFINEMENT8 (2008) 096.
- [37] I. Adachi *et al.* (Belle Collaboration), arXiv:0810.0358.
- [38] O. Zhang, C. Meng, and H. Q. Zheng, arXiv:0901.1553.
- [39] S. Flatté, Phys. Lett. B **63**, 224 (1976).
- [40] M. B. Voloshin, Phys. Lett. B **579**, 316 (2004).
- [41] V. Baru *et al.*, Phys. Lett. B **586**, 53 (2004).
- [42] S. Dubynskiy and M. B. Voloshin, Phys. Rev. D **77**, 014013 (2008).
- [43] D. Bugg, J. Phys. G **35**, 075005 (2008).
- [44] C. Meng, Y. J. Gao, and K. T. Chao, arXiv:hep-ph/0506222.
- [45] S. Weinberg, Phys. Rev. **130**, 776 (1963); **131**, 440 (1963); **137**, B672 (1965).
- [46] D. Morgan, Nucl. Phys. A **543**, 632 (1992).
- [47] E. Braaten and M. Lu, Phys. Rev. D **76**, 094028 (2007).
- [48] C. Hanhart, Yu. S. Kalashnikova, and A. V. Nefediev (unpublished).
- [49] M. Nauenberg and A. Pais, Phys. Rev. **126**, 360 (1962).
- [50] E. Braaten and J. Stapleton, arXiv:0907.3167.